
Chapter 7

Gas filled interrupters – fundamentals

G.R. Jones

7.1 Introduction

The interruption of current in a network cannot meaningfully be considered in isolation from the operating voltage of the system and the nature of the system components and structure. The operating voltage itself affects the type of interrupter chosen for duty whilst the system components and structure (e.g. the extent to which the network is inductive etc.) will influence the detailed design of the interrupter unit because of the voltage transients produced during the current interruption process. It is for these reasons that a discussion of current interruption in electric power systems is appropriate in a book on high voltage technology.

The discussion is mainly about SF₆ interrupters since this medium is the only serious contender for use in circuit-breakers across the entire range of medium, high and extra high voltages. Other contenders – air, oil and vacuum – have an inferior voltage withstand capability (Figure 7.1), although this is not an exclusive consideration with regard to current interruption and there are ranges in which vacuum, in particular, can offer advantages.

The fundamental principles of current interruption as governed by high voltage considerations are therefore described with respect to both system based effects and the characteristics of circuit-breakers. Various types of SF₆ interrupters are considered and different factors which limit their performance are explained. Some possible trends in future developments are indicated.

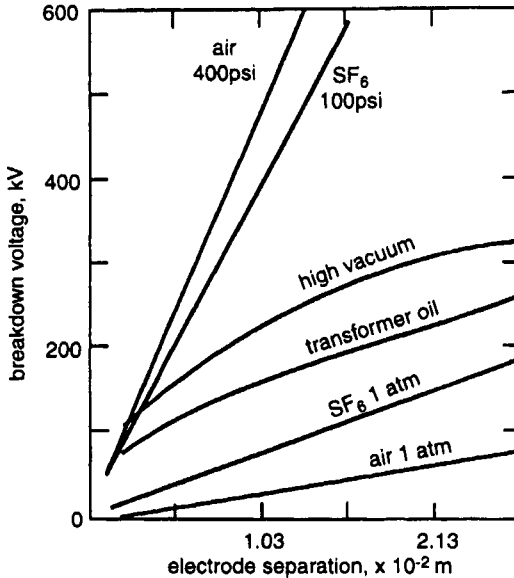


Figure 7.1 Breakdown voltages of various interrupter media

7.2 Principles of current interruption in HV systems

All methods of interrupting current in high voltage systems rely on introducing a nonconducting gap into a metallic conductor. To date, this has been achieved by mechanically separating two metallic contacts so that the gap so formed is either automatically filled by a liquid, a gas or even vacuum. In practice, such inherently insulating media may sustain a variety of different electrical discharges which then prevent electrical isolation being achieved.

There are three major facets to such electrical discharges which then prevent electrical isolation being achieved. First, as contacts are separated, an arc discharge is inevitably formed across the contact gap. The problem of current interruption then transforms into one of quenching the discharge against the capability of the high system voltage of sustaining a current flow through the discharge. Since this physical situation is governed by a competition between the electric power input due to the high voltage and the thermal losses from the electric arc, this phase of the current interruption process is known as the 'thermal recovery phase' and is typically of a few microseconds' duration.

The second facet of current interruption relates to the complete removal of the effects of arcing which only occurs many milliseconds after arc formation even under the most favourable conditions. The problem then is one of ensuring that the contact geometry and materials are

capable of withstanding the highest voltage which can be generated by the system without electrical breakdown occurring in the interrupter.

The third facet bridges the gap between the thermal recovery phase and the breakdown withstand phase. The problem in this case is that the remnant effect of the arcing has cleared sufficiently to ensure thermal recovery but insufficiently to avoid a reduction in dielectric strength. This is known as the 'dielectric recovery phase'.

Based on this understanding, circuit interruption technology is concerned on the one hand with the control and extinction of the various discharges which may occur, whilst on the other it relates to the connected system and the manner in which it produces post-current interruption voltage waveforms and magnitudes.

7.2.1 System-based effects

The basic premise which derives from the above considerations, as far as system effects are concerned, is that it is advantageous for the current to be reduced to zero in a controlled manner. The simplest and most common example is the symmetrical power frequency (50 Hz) current wave since the current reduces naturally to zero once every half-cycle (Figure 7.2) and at which point current interruption is sought. This represents the minimum natural rate of current decay (di/dt) so that for conventional power systems, which are inherently inductive, the induced voltage following current interruption is minimised. Consequently, the contact gap is less severely stressed transiently during both the thermal and dielectric recovery phases.

The voltage transients of most interest in interrupting current in high voltage transmission systems are those produced by short-circuit faults

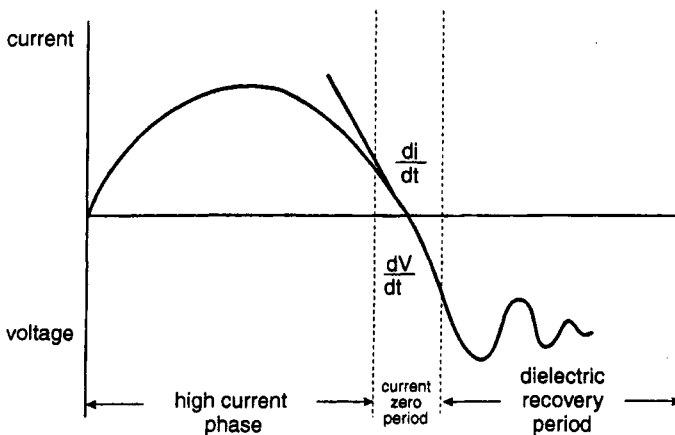


Figure 7.2 Voltage and current waveforms during the current interruption process

and short line faults. Short-circuit faults occur close to the circuit-breaker (Figure 7.3). These produce the most onerous fault currents. In this case, the restrike voltage consists of a high frequency (ω_n) oscillation (governed by the system inductance (L) and capacitance (C)) superimposed on an exponentially decaying component governed by the system resistance (R):

$$V_c \approx V_o [1 - e^{-R/2L t} \cos \omega_n t]$$

The maximum fault current is (e.g. Reference 1)

$$I_F \approx \frac{V_o}{\omega L} \sin \omega t$$

and the maximum possible voltage across the circuit-breaker is twice the supply voltage. The system resistance R reduces this maximum voltage to lower values.

Short line faults occur on transmission lines a few kilometres from the circuit-breaker (Figure 7.4) and constitute the most onerous transient recovery voltages. The voltage across the circuit-breaker is the sum of the line side (V_L) voltage and the source side (V_s) voltage which occur at two different frequencies f_L and f_s , respectively (Figure 7.4). Typically, at current zero (dV/dt) $\approx 10\text{--}20 \text{ kV}/\mu\text{s}$.

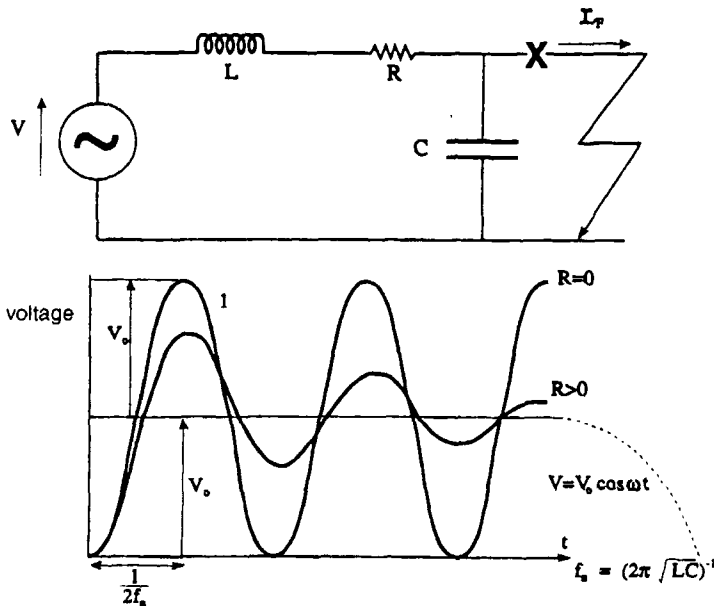


Figure 7.3 Short line fault – onerous fault current

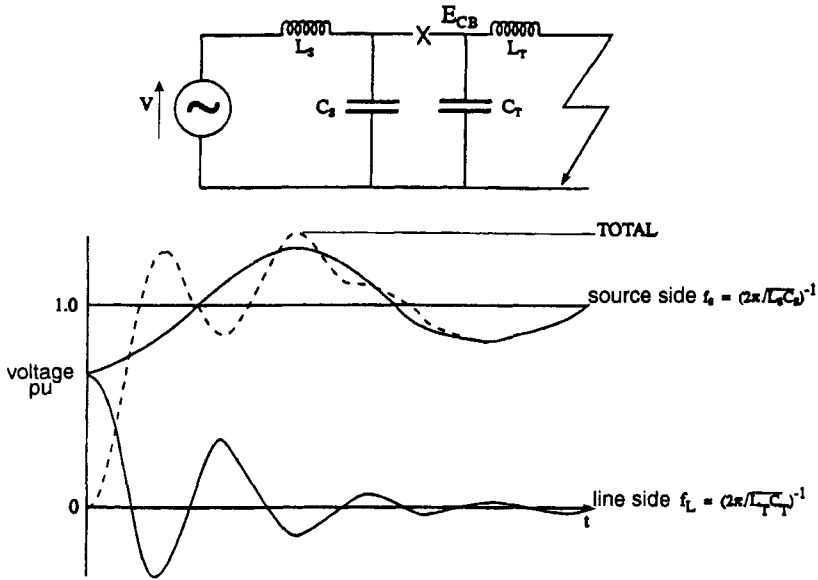


Figure 7.4 Short line fault – onerous transient recovery voltages

The situation is made more complicated in three-phase systems because current zero occurs at different times in each phase, implying that the fault is interrupted at different times leading to different voltage stresses across the interrupter units in each phase.

Apart from the symmetrical sinusoidal current waveform with its natural current zero, other current interruption situations exist (Figure 7.5). For instance, the sinusoidal waveform may be superimposed on a steady current to form an asymmetric wave with major and minor loops which cause different circuit-breaker stresses. A related condition which occurs in generator faults corresponds to the power frequency wave superimposed on an exponentially decaying component (Figure 7.5) so that zero current crossing may be delayed for several half-cycles. A further situation is the interruption of DC faults which is achieved by inducing an oscillatory current via arc instability in the circuit-breaker and so forcing the current to pass through zero eventually (Figure 7.5).

At the lower domestic voltages, current limitation can be conveniently induced leading to an earlier and slower approach to zero current than occurs naturally and with the additional benefit of reducing the energy absorption demands made of the interrupter module (Figure 7.5).

Finally, there are situations whereby high frequency (kHz–MHz) currents can be induced and these need to be tolerated by the circuit-breaker. These occur, for instance, when switching on load inductors so

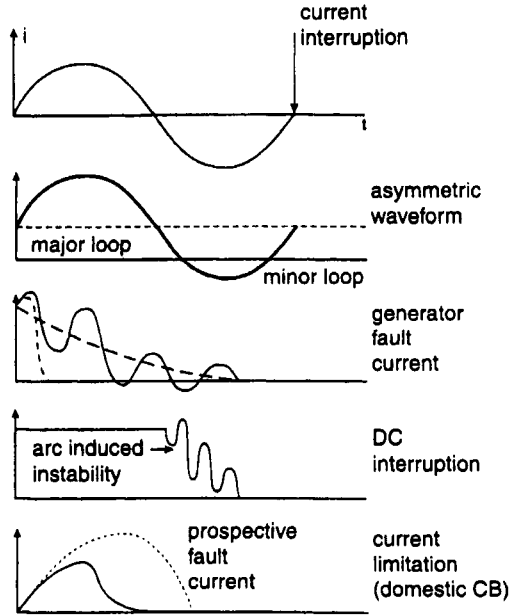


Figure 7.5 Circuit-breaker current waveforms

that the line-side considerations on Figure 7.4 are replaced by a lumped inductor load.

7.2.2 Circuit-breaker characteristics

The basic characteristics of a circuit-breaker relate respectively to the thermal and dielectric recovery phases.

The thermal recovery characteristic is in the form of a critical boundary separating fail and clear conditions on a rate of rise of recovery voltage (dV/dt) and rate of decay of current (di/dt) diagram (Figure 7.6a).

Typically, the boundary obeys the relationship:

$$\frac{dV}{dt} = \text{const.} \left(\frac{di}{dt} \right)^n$$

with $n = 1 - 4.6$.

The thermal recovery performance may be improved by increasing the pressure of the circuit-breaker gas, the nature of the gas or the geometry of the interrupter head (Figure 7.6 b).

For the dielectric recovery regime the characteristic is represented by

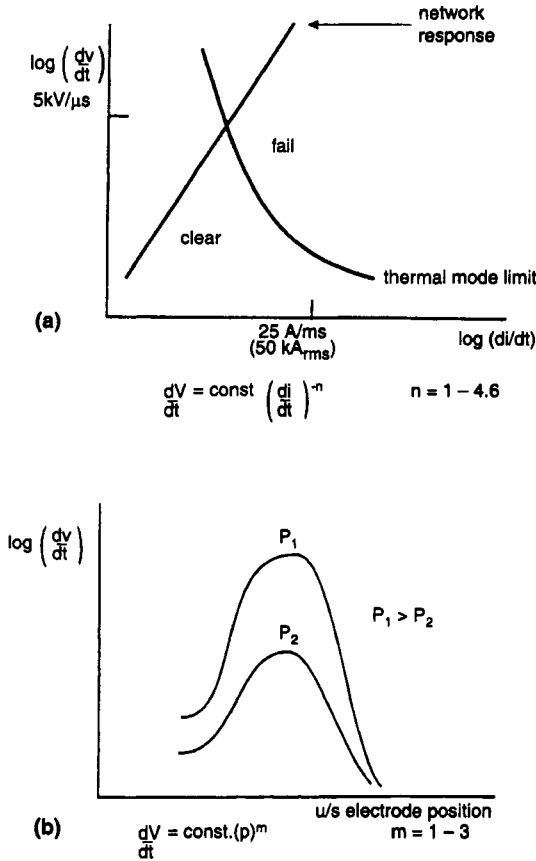


Figure 7.6 Thermal recovery characteristics
 (a) Network response and interrupter characteristic
 (b) Effect of pressure and geometry on performance

the critical boundary separating successful clearance and fail on a maximum restrike voltage (V_{MAX}) and rate of decay of current (di/dt) diagram (Figure 7.7). The dielectric recovery performance may be improved by increasing the number of contact gaps (interrupter units) connected in series. By combining the thermal and dielectric recovery characteristics, the overall limiting curves for circuit-breaker performance are obtained (Figure 7.8).

7.3 Arc control and extinction

The essence of good circuit-breaker design and operation is to ensure proper arc control and efficient arc quenching to provide rapid voltage withstand capability after current interruption. This, in turn, relies on the

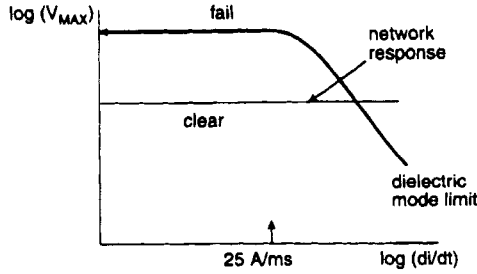


Figure 7.7 Dielectric recovery characteristic

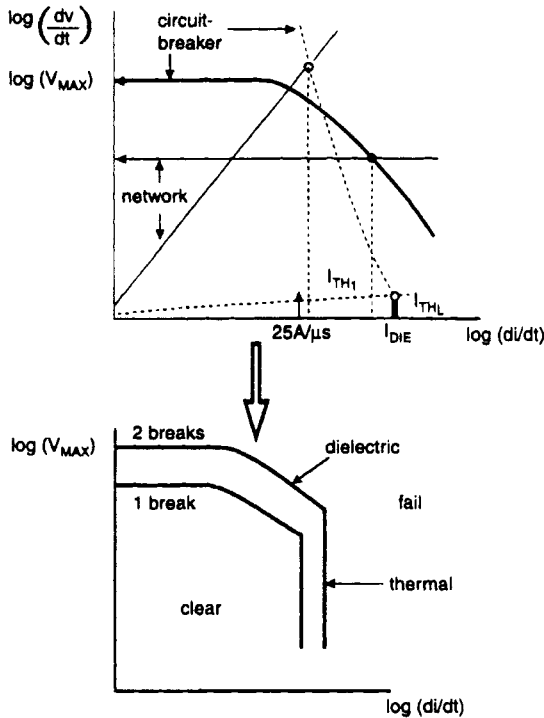


Figure 7.8 Overall circuit-breaker performance – superposition of thermal and dielectric

removal of power dissipated in the arc discharge by Joule heating via the processes of convection, conduction and radiation (Figure 7.9). They may be enhanced through the choice of arcing medium (e.g. sulphur hexafluoride) and arc confinement/movement method.

The properties of SF₆ with regard to high breakdown voltage, enthalpy removal capability and compressive effects have made it an almost universal choice for extra high voltage applications. The influence

7.3.1 Gas blast circuit-breakers

In gas blast circuit-breakers the contacts are separated along the axis of a gas flow guiding nozzle so that the arc is subjected to the convective effects of a co-axial gas flow (Figure 7.11). The gas flow is produced by gas compression upstream of the nozzle.

Rather than storing gas indefinitely at high pressure until a fault demands attention, the trend has been to compress the gas transiently by piston action ('bicycle pump') simultaneous to contact separation when fault interruption is required. This is the principle of the 'puffer circuit-breaker', which may be configured with two nozzles in tandem, back to back, to provide a duoflow or, if the nozzles are of a different size, a partial duo flow unit.

The thermal recovery performance of such circuit-breakers is governed by the empirical relationship (Figure 7.12):

$$\left[\frac{dV}{dt} \right]_{CRIT} = ap^{1.5}(1 + 1.7\Delta p)A_o^{1.5} \left(1 + (5 \times 10^{-5} \hat{f}) \left(\frac{di}{dt} \right)^2 \right)^{-1} \quad (7.1)$$

Typical pressure time curves are shown on Figure 7.13.

The required gas compression may also be generated by relying on arc induced gas heating to produce the pressurisation within a confined volume according to the gas law:

$$p = \left(\frac{R}{V} \right) T \quad (7.2)$$

where V = volume, T = gas temperature and R = gas constant.

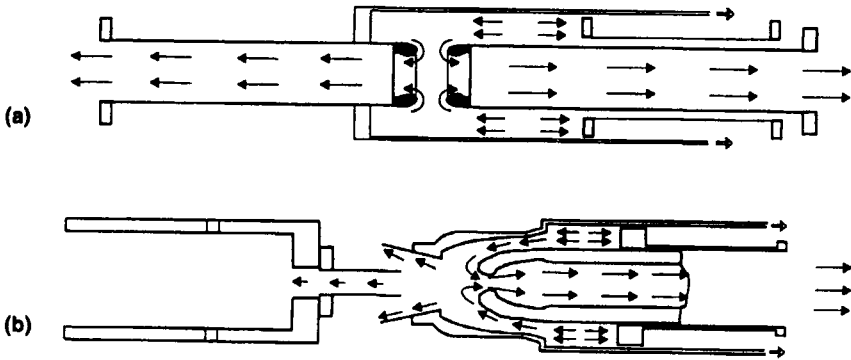


Figure 7.11 Gas blast interrupters
 (a) Duo blast
 (b) Partial duo blast

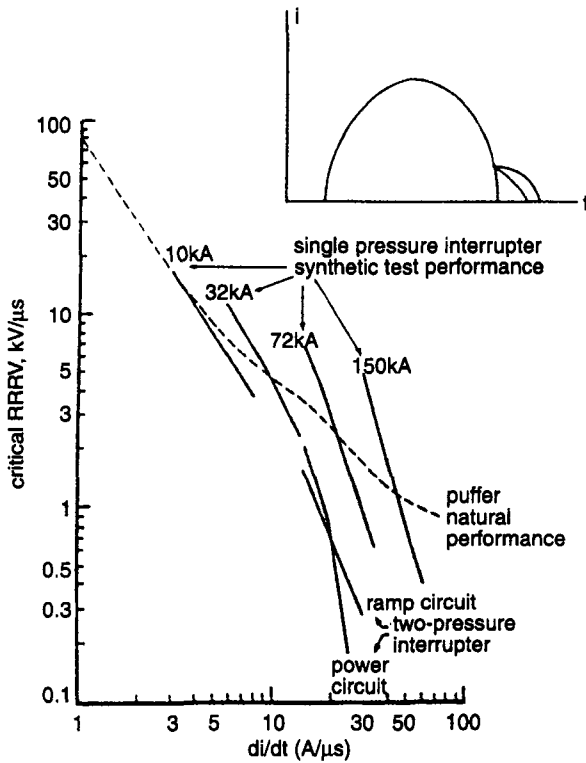


Figure 7.12 Effect of various parameters on the thermal recovery characteristics of gas blast interrupters

The pressurisation produced at the end of a half-cycle of fault current depends on the parameter [3]:

$$Y = \frac{J_o (1 - \alpha) Il}{a, \sigma \omega U_o(t)} \tag{7.3}$$

where

- α = fraction of input power transferred by radiation
- σ = electrical conductivity of arc plasma
- l = effective length of the arc
- $U_o(t)$ = time varying volume of the arc chamber
- \hat{I} = peak current
- ω = angular frequency of current waveform

as shown in Figure 7.14.

The thermal recovery performance is governed by eqn 7.1 with the piston pressure term set to unity. The manner in which piston and arc induced pressures affect the thermal recovery performance of the circuit-breaker is shown in Figure 7.12.

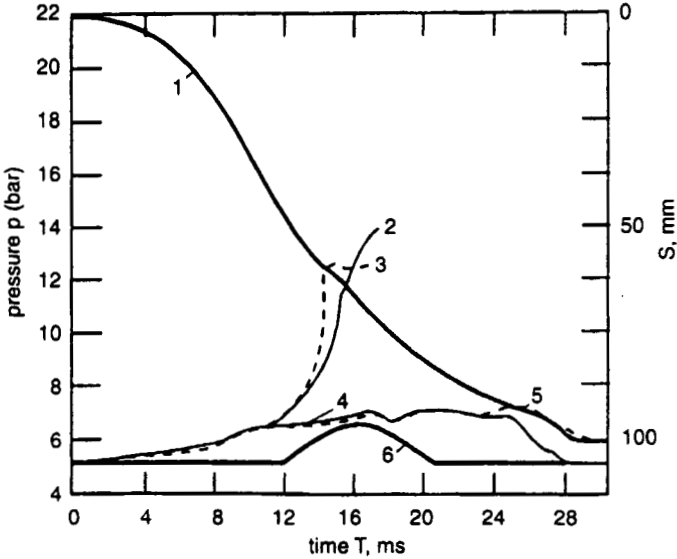


Figure 7.13 The pressure inside the puffer chamber
 1: piston stroke curve;
 2, 3: calculated and measured chamber pressure for a peak of 18.6 kA;
 4, 5: calculated and measured chamber pressure in the absence of the arc;
 6: current waveform

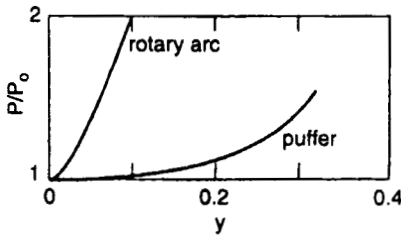


Figure 7.14 Arc-induced pressure elevation as a function of volume normalised current
 $y = (J_u(1 - \alpha) \hat{I}) / (.a, \sigma \omega U_u(t))$

7.3.2 Electromagnetic circuit-breakers

In electromagnetic circuit-breakers the arc is spun through the action of the Lorentz force produced by the fault current flowing through a *B* field producing coil. The arc may be spun azimuthally or helically (Figure 7.15). By contrast with the gas blast circuit-breakers, arc controlling and quenching convection is generated by driving the arc through the surrounding flow rather than vice versa.

The thermal recovery performance is typically governed by [2] (Figure 7.16)

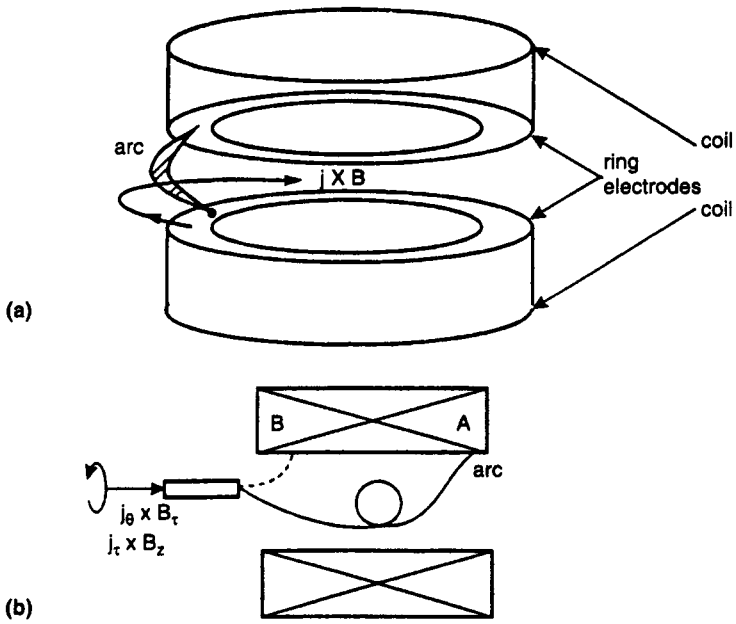


Figure 7.15 Electromagnetic interrupters
(a) Rotating arc, (b) helical arc

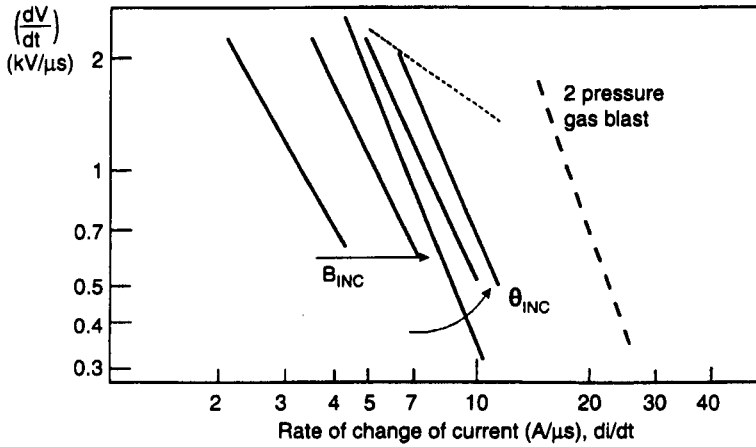


Figure 7.16 Effect of various parameters on the thermal recovery characteristics of rotary arc interrupters
—— constant B - - - - - particular unit

$$\left[\frac{dV}{dt} \right]_{CRIT} = ap^{1.5} \left(\frac{di}{dt} \right)^n B^{1.9} f(\theta) \quad (7.4)$$

where B = magnetic flux density.

The phase angle between i and B for a helical arc interrupter is governed by [2]

$$\tan \theta = \frac{\omega L_T l_T \Delta}{\zeta_T \pi d} \quad (7.5)$$

where ω is the angular frequency, L_T , ζ_T are the self-inductance and resistivity of the material of the annular contact, and l_T , Δ , d are the length, thickness and diameter of the cylindrical contact, respectively.

The typical performance curves given in Figure 7.16 are for constant B , whereas in practice B increases with fault current level. The characteristic for a given interrupter therefore forms a locus across the constant B curves (much as the characteristic for the puffer breaker forms a locus across the constant pressure curves of Figure 7.12). Note the similar gradients of the electromagnetic and gas blast characteristics.

7.3.3 Dielectric recovery

The dielectric recovery in SF_6 gas is a complex process governed by the dissociation chemistry of SF_6 which is only partially understood. Theoretical estimates of the time variation of concentration of dissociation by-products following arcing (and based on unconfirmed equilibrium assumptions) show the complexity of the medium when subjected to voltage stresses (Figure 7.17a). The temperature of the dissociated SF_6 in the post arc column is deduced to recover via a number of steps which are governed by the thermal capacity and conduction properties of the dissociated by-products.

Estimates of the recovery of dielectric strength then yield characteristics of a step-like nature as shown in Figure 7.17b. The evidence is that the precise nature of this curve is affected by the shape of the restriking voltage waveform because of the influence of the associated electric field on the recombination chemistry of the ionic species.

7.4 Other performance inhibiting factors

What has been described above are the fundamental factors which govern circuit-breaker performance under almost ideal situations. For instance, the circuit-breaker thermal recovery characteristics of Figures 7.12 and 7.15 are, in principle, predictable from the physics shown in

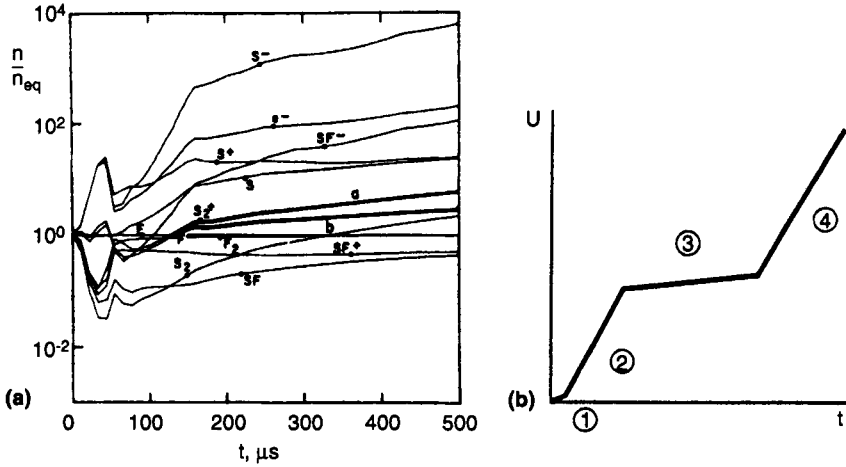


Figure 7.17 Dielectric recovery characteristics
 (a) SF_6 dissociation products during dielectric recovery
 (b) Voltage withstand as a function of time

Figure 7.9 using the laws of conservation of mass, momentum and energy – provided the boundary conditions and material properties are known.

However, in practice, complicating effects arise from a lack of knowledge of the material properties (e.g. enthalpy, radiation transport, etc.) of the arcing medium which follows from the complex dissociation chemistry (Figure 7.10 and 7.17a) and the entrainment of foreign species from, for example, the interrupter contacts and nozzle and affecting the fundamental plasma properties in a complicated manner.

In addition to these factors additional complex phenomena have emerged which without proper designs may limit the performance of SF_6 circuit-breakers in other ways.

7.4.1 Particulate material

The arc induced dissociation of the SF_6 , the evaporation of contact material and the ablation of PTFE from the nozzle all lead to a complicated chemical situation from which a number of solid particle materials can be shown to be formed.

At high current levels the tungsten from the sintered copper–tungsten contacts may be ejected as particles on account of the tungsten's higher evaporation temperature than copper, leaving it as a fragile matrix after the copper has evaporated. The presence of such particulate tungsten has been detected spectroscopically and its persistence in the contact gap of an interrupter can lead to the interrupter failing to interrupt the fault current (Figure 7.18). However, such effects can be minimised via the

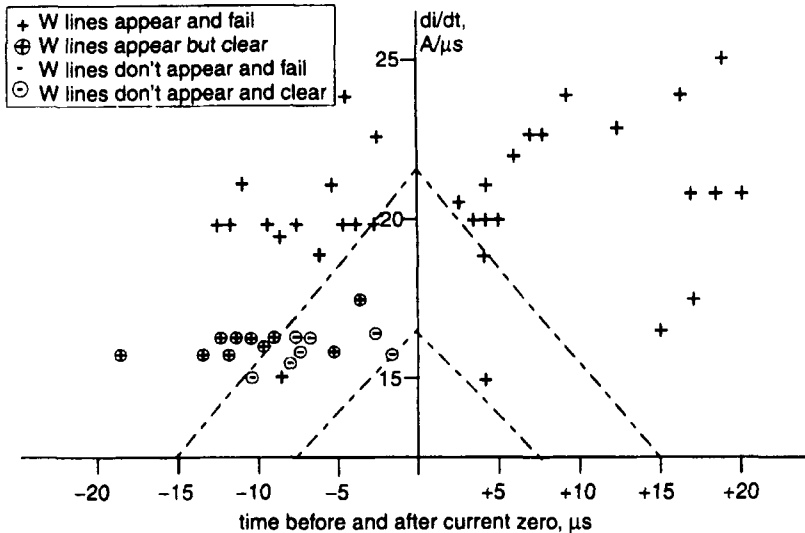


Figure 7.18 Correlation between thermal recovery failure and the presence of tungsten in the arc plasma at current zero for various values current decay rate (di/dt)
gas pressure = 60 pounds per square inch gauge ($p = 60$ psig)

introduction of the duo flow interrupter geometry which produces a flushing action of the contact gap because of the resulting contraflow. There is experimental evidence that luminous particles may persist for long periods in SF_6 , possibly due to some chemical reactivity so that, although such particles may be removable from the contact gap, they may nonetheless exist for longer times within the circuit-breaker tank. As a consequence these particles may degrade the dielectric recovery of the interrupter by reducing the voltage withstand capability (Figure 7.19). There is evidence that it may be these particles rather than the overheating of the SF_6 by intense arcing which may dominate in governing the dielectric performance limit.

In addition to these luminous particles, nonluminous particles are also formed following arcing. Their properties and influence are less well understood than the luminous particles but there is some experimental evidence that they may carry electrical charges which because of the low mobility of the particles may persist for long periods within the circuit-breaker tank.

7.4.2 High frequency transients

There are at least two high frequency effects which occur in interrupters and isolators and which may affect the current interruption process.

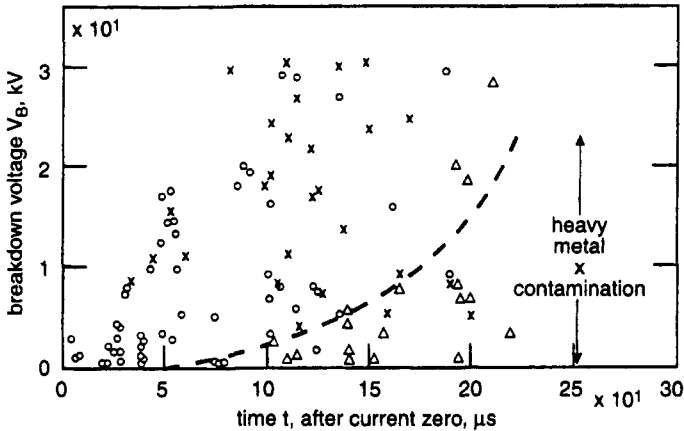


Figure 7.19 Effect of particulate material on dielectric recovery

The first relates to the formation of fast transients in gas insulated substation (GIS) systems. These are high frequency (kHz) electromagnetic waves which propagate within the SF₆ containing busbar modules of such systems. They are only slowly attenuated because of the low-loss nature (low R in Figure 7.3) of the co-axial GIS which act essentially as waveguides. One of the sources of such transients is pre-arcing during the closing operation of an isolator or interrupter. Optical investigations of such switch operation have shown that events on the timescale of GHz may occur and that reflected waves within the GIS system interact to feed energy back into the arc which has insufficient time to be self-quenching (Figure 7.20).

A second situation where high frequency arcing occurs is during on-load inductor or capacitor switching. In this case, arcing at frequencies in excess of kHz may occur during the closing or opening operations but at peak currents of only a few hundred amperes.

The effects are probably associated with network resonances close to the interrupter. In terms of the thermal recovery characteristics of Figure 7.12 the implication is that although the peak current is low the di/dt at current zero is high (due to the high frequency of the waveform) and typically lies off the (di/dt) axis of Figure 7.12 at the high di/dt end.

Consequently, the voltage withstand and capability to interrupt is exceedingly low according to the characteristics of Figure 7.12, so that the interrupter will tend to fail to interrupt such high frequency currents. Furthermore, the high di/dt at current zero coupled with the inductive nature of the load is inclined to produce high restriking voltages, which may exceed the rating of the circuit-breaker.

Evidence is now emerging that such high frequency phenomena within the interrupter unit may lead to unusual breakdowns which occur away

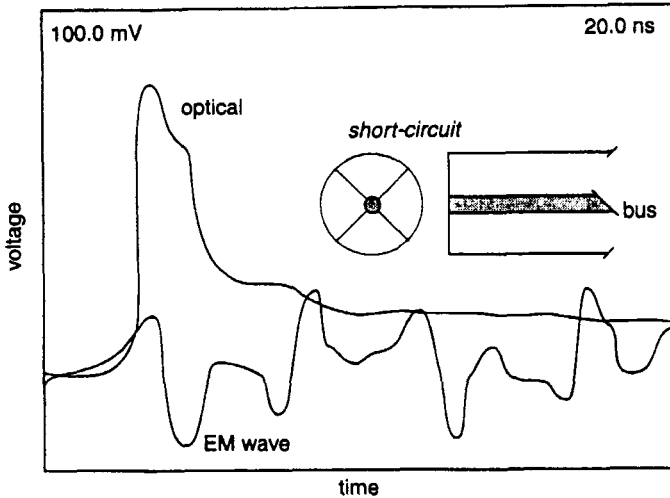


Figure 7.20 Coupling between high frequency electromagnetic transients and an arc in an isolating switch

from the main contact gap. This constitutes a serious situation since the potential for extinguishing the discharge by the normal operation of the interrupters no longer exists, leading to the possibility of the interrupter unit itself being damaged or destroyed.

7.4.3 Trapped charges on PTFE nozzles

Experimental investigations [4, 5] have indicated that electric charges may be trapped on and migrate along the surface of PTFE nozzles. As a result the electric field distribution within the interrupter head is distorted (Figure 7.21), becoming concentrated so that with the appropriate voltage polarity on the contacts, electrical breakdown is enhanced along the external wall of the nozzle. The probability of the electrical breakdown occurring outside the nozzle depends on the moving contact position with respect to the exit of the PTFE nozzle as shown on Figure 7.22 [5]. There is evidence that as a result electrical discharge puncturing may occur through the wall of the PTFE nozzle.

The decay of electric charge on the surface of PTFE is considerably slower than on other polymeric materials and under some conditions may remain conserved for over 400 days (Figure 7.23). Such prolonged charge preservation would appear to be a contributory reason for late voltage restrikes which may occur across open contact gaps with some interrupters under particular conditions.

To overcome such effects and improve interrupter performance different types of PTFE materials loaded with different impurities may be utilised in more recent interrupter units.

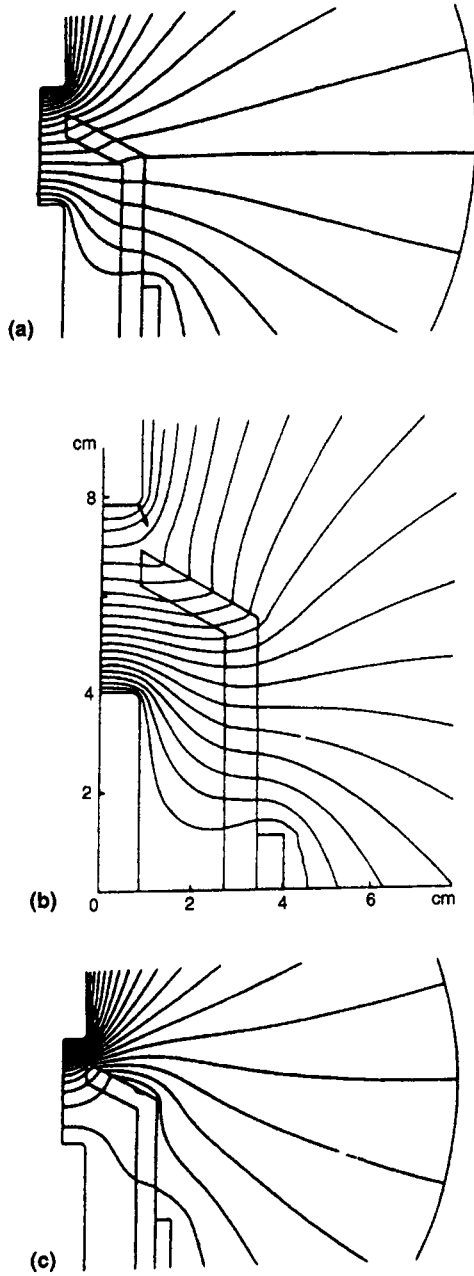


Figure 7.21 Electric field distribution around a PTFE nozzle
(a) No surface charge
(b) $+20 \mu\text{C}$ surface charge
(c) $-20 \mu\text{C}$ surface charge

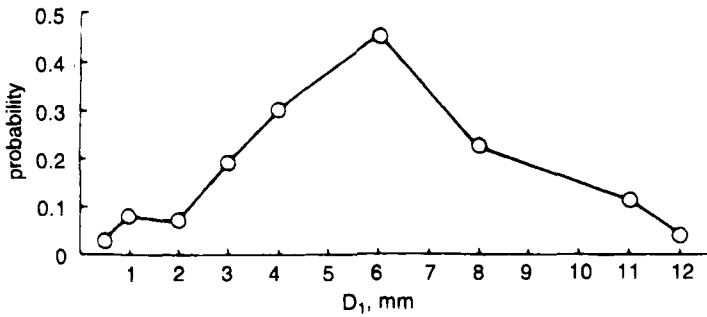


Figure 7.22 Probability of electrical breakdown outside a PTFE nozzle of particular geometry as a function of the moving contact separation – nozzle mouth D_1

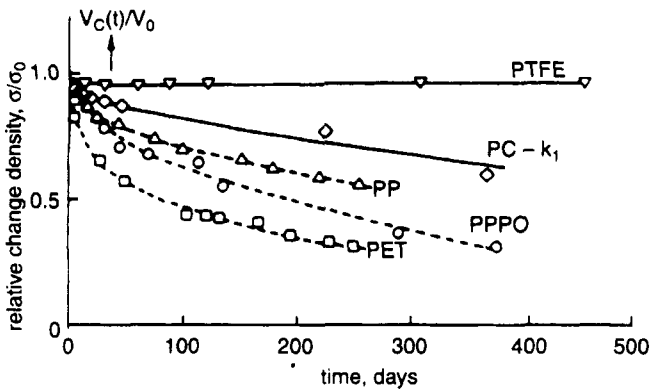


Figure 7.23 Charge decay in dry atmosphere at room temperature for various electrets [5]

- ∇ 50 μm Teflon (PTFE)
 - \diamond 25 μm polycarbonate (PC- k_1)
 - \triangle 20 μm polypropylene (PP)
 - \circ 25 μm poly-2,6-diphenyl-1,4-phenyleneoxide (PPPO)
 - \square 25 μm Maylar (PET)
- All electrets are thermally charged

7.5 Other forms of interrupters

7.5.1 Domestic circuit-breakers

Lower voltage circuit-breakers such as those used at domestic (250 V) and industrial voltages utilise air as the main arc quenching medium in combination with a linear electromagnetic drive. The arc is formed between two parallel contacts and driven along these by the electromagnetic force produced by the fault current itself (Figure 7.24), ultimately

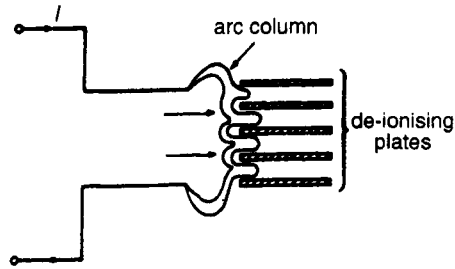


Figure 7.24 Domestic circuit-breaker with de-ionising plates

being forced into narrow gaps between a stack of de-ionising plates. The arc is extinguished by the plates absorbing energy from the arc plasma and through the formation of a series of separate arcs between the plates. The formation of a number of anodes and cathode spots on the plates increases the voltage drop across the series of electric arcs and because of the limited supply voltage produces current limitation and ultimate extinction, as already shown in Figure 7.5.

7.5.2 Oil filled circuit-breakers

Oil filled circuit-breakers have been widely used at distribution voltage levels and many remain in use today. In these interrupters arc quenching is achieved by the oil absorbing energy from the arc plasma, causing it to locally evaporate and so form a gas bubble with good arc extinguishing properties. In some designs there may be a lateral flow oil and the arc driven onto a series of de-ionising vanes similar to the domestic circuit-breaker arrangement (Figure 7.25).

7.5.3 Vacuum interrupter

The vacuum interrupter differs fundamentally from the other types of interrupters in that the arc plasma is diffuse and does not rely on a surrounding medium from which to absorb energy [6]. Instead the arc is sustained by the emission of electrons and ions from the circuit-breaker contacts. Current interruption occurs at current zero if the supply of such ions and electrons can be sufficiently rapidly ceased and those already in the contact gap removed. Metal vapour condensing shields may be used to assist the process (Figure 7.26). Thus the successful operation of such an interrupter relies on the prevention of a constricted arc column and electrode spots being formed. This may be assisted through the use of contact designs which rapidly move the arc roots electromagnetically.

Such interrupters are mainly confined to distribution voltage levels since in practice it is difficult to move contacts sufficiently far apart under

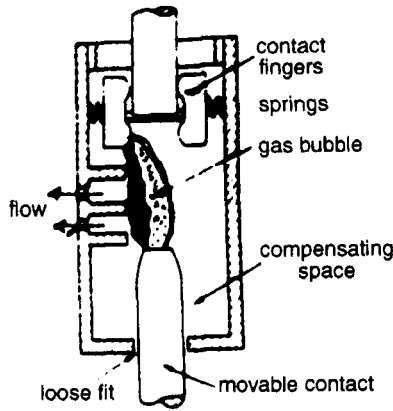


Figure 7.25 Oil circuit-breaker
Oil circuit-breaker losses enhanced by thermal capacity of oil

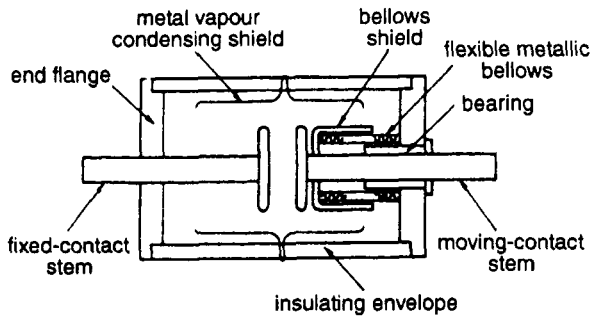


Figure 7.26 Cross-section of a vacuum interrupter

the necessary high vacuum conditions because of restrictions produced by vacuum sealing.

7.6 Future trends

The advent of SF₆ circuit-breakers has led to significant commercial benefits:

- (a) At EHV, the interruption capability per interrupter unit has increased significantly (Figure 7.27), and incorporation into gas insulated systems is facilitated. The net effect is to reduce substation size with accompanying reduction in land costs.
- (b) At distribution level, rotary arc circuit-breakers have better immunity to current chopping than other types of circuit-breakers.

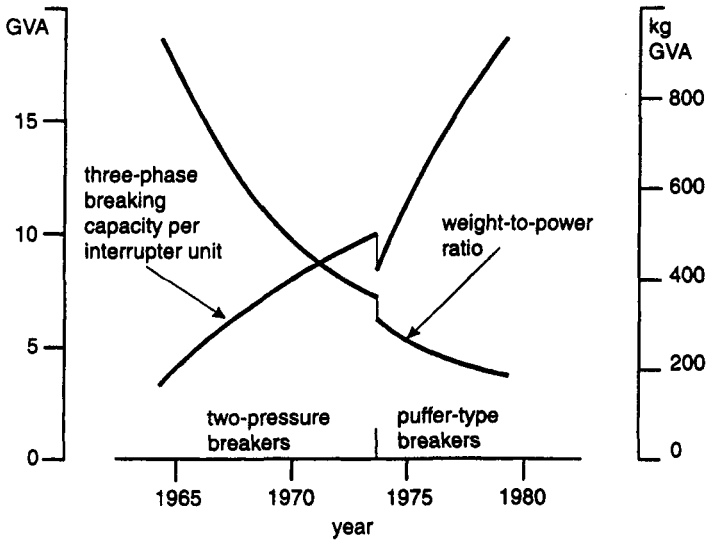


Figure 7.27 Development of SF₆ circuit-breakers

However, these advantages have been gained only at the expense of other aspects. For instance, the puffer circuit-breaker makes expensive demands on operating energy (Figure 7.28) because of the rapid piston action which is needed, and the trend is to evolve designs which are less energy demanding.

The move towards various degrees of self-pressurisation by arc-induced gas heating is an example of such a trend. However, the least energy demanding operation is with the electromagnetic type of circuit-breakers so that considerations of extending such principles to higher voltage levels is receiving some attention.

A number of aspects regarding electromagnetically spun arc interrupters are emerging which may impact on future design considerations:

1. Electromagnetically driven helical arcs (Figure 7.15b) have the capability to pump gas along the axis of the tube formed by the annular contact via one of two mechanisms. The first mechanism results from the 'fan action' of the rotating arc inclined at an angle ϕ to the annular contact axis (Figure 7.29). The mass flow rate produced by the fan action is [7]

$$\dot{m} = \pi b^2 \rho \sin \phi (\pi w^2 a z \sin \phi)^{1/2} \quad (7.6)$$

where a is the arc column radius, b is the radius of the annular contact, z is the extent of the axial displacement of the arc root on

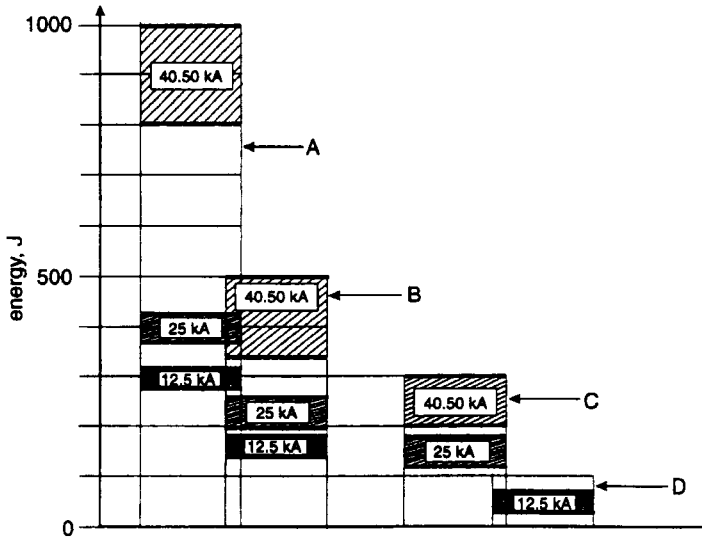


Figure 7.28 Evolution of opening energy as a function of the interrupting technique used and the interrupting capacity expressed in kA. The increasingly simple design and the utilisation of the arc energy result in a reduction in switching energy.

- (A) Auto-pneumatic technique
- (B) Auto-pneumatic + thermal expansion technique
- (C) Thermal expansion + rotating arc technique
- (D) Thermal expansion or rotating arc technique

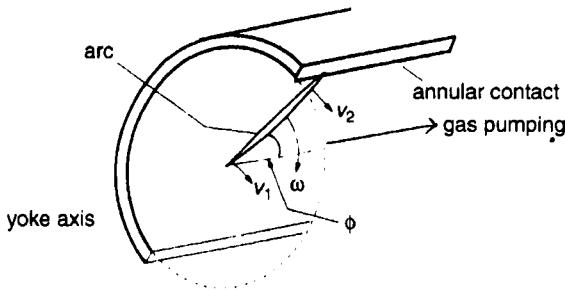


Figure 7.29 Gas pumping due to arc fan action

the annular contact, w is the rotational speed of the arc column and ρ is the ambient gas density.

The second pumping mechanism results from the reciprocating action of the arc helix penetrating axially into the annular contact and regularly short-circuiting itself (Figure 7.15b). The mass flow rate produced by this piston action is [7]

$$\dot{m} = \rho s(2a)[(2Bi_c)/(\rho(2a)C_D)]^{1/2} \quad (7.7)$$

where s is the circumferential length of the arc column, B is the driving magnetic flux density, i_c is the circumferential component of the arc current and C_D is the drag factor.

Mass flow rates of the order of 0.2 kg s^{-1} are produced by each mechanism, the ‘fan action’ dominating for lower arc rotation speeds whilst the ‘piston action’ dominates at higher speeds (Figure 7.30).

The significance of such gas pumping action is that the SF_6 dielectrically weakened by arc overheating locally is removed by this induced unidirectional flow from the dielectric sensitive localities within the interrupter.

2. A limitation of self-excited rotary arc circuit-breakers which rely on the fault current to produce the Lorentz driving force is that it is difficult to design cover for all operating conditions. Since the Lorentz force with a self-excited coil varies as the square of the fault current but with a separately excited coil the variation with fault current would be only linear, it is possible to better provide a higher arcing driving force with the latter for low fault current interruption. For instance, with coil exciting currents of 100–500 A equivalent driving forces to self-excitation can be produced for 2–10 kA fault currents, whilst an order of magnitude greater driving force is produced for a 100 A fault current level (Figure 7.31). In addition to producing enhanced interruption capabilities at lower fault currents,

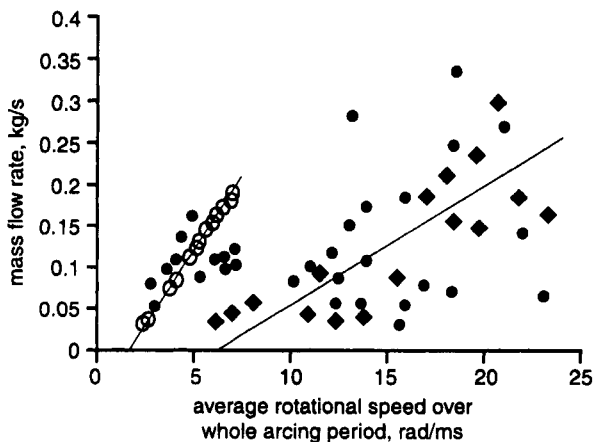


Figure 7.30 Mass flow rates of gas produced by fan and piston action of an electromagnetically driven helical arc [7]

- experiment
- arc fan
- ◆ arc piston

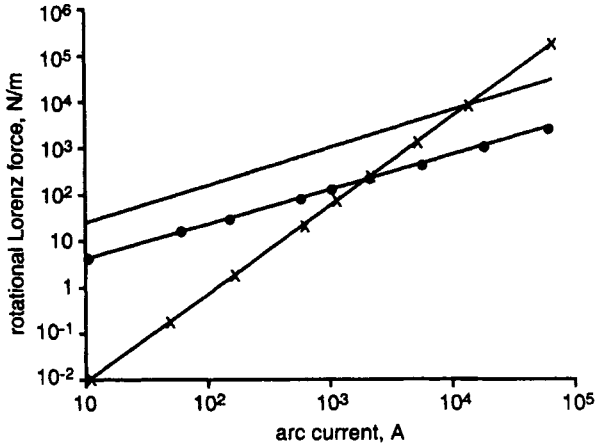


Figure 7.31 Rotational Lorentz force produced by self- and separate excitation of the B field producing coil as a function of arc fault current [7]

— x — series
 — • — ind. 100A
 — • — ind. 500A

separate coil excitation also leads to less severe demands on the electromechanical design of the B field producing coil.

Profiling the B field distribution within and around the annular contact volume, through the use of two separately switched coils, can also produce increased power losses from the arc plasma column leading to improved current interruption [8].

Finally, there are also issues relating to environmental aspects arising from the greenhouse effect capabilities of SF₆. The need to control SF₆ usage is likely in the future to influence the development of new circuit-breakers, but attempts over many years to find suitable replacements for SF₆ have not been successful.

7.7 References

1. JONES, G.R.: 'High pressure arcs in industrial devices' (Cambridge University Press, 1988)
2. RAGALLER, K. (Ed.): 'Current interruption in HV networks' (Plenum Press, 1978)
3. RYAN, H.M. and JONES, G.R.: 'SF₆ switchgear' (Peter Peregrinus Ltd, 1989)
4. LIU, W.D., SPENCER, J.W. WOOD, J.K. CHAARAOUI, J.J. and JONES, G.R.: 'Effect of PTFE dielectric properties on high voltage reactor load switching', *IEE Proc Sci Meas Technol*, 1996, **143**, (3), pp. 195–200

5. LIU, W.D., CHAARAOUI, J., WOOD, J.K., SPENCER, J.W. and JONES, G.R.: 'Parasitic arcing in EHV circuit-breakers', *IEE Proc. A* 1993, **140**, (6), pp. 522–528
6. GREENWOOD, A.: 'Vacuum switchgear' (Institution of Electrical Engineers, 1994)
7. ENNIS, M.G., JONES, G.R., KONG, M.G., SPENCER, J.W. and TURNER, D.R.: 'A rotating arc gas pump for circuit-breaking and other applications', *IEEE Trans. Plasma Sci.*, 1997, **25**, pp. 961–966
8. ENNIS, M.G., SPENCER, J.W., TURNER, D.R. and JONES, G.R.: 'A low current electromagnetically driven arc discharge in SF₆'. Proc XIIth Int. Conf. on *Gas discharges and their applications*, Greifswald, Germany, 1997